Immunoasssay based on the antibody-conjugated PAMAM-dendrimer–gold quantum dot complex†

Robert C. Triulzi,[a] Miodrag Micic,*[b] Silvia Giordani,[c] Michael Serry,[d] Wen-An Chiou[e] and Roger M. Leblanc*[a]

Received (in Cambridge, MA, USA) 4th August 2006, Accepted 26th October 2006
First published as an Advance Article on the web 21st November 2006
DOI: 10.1039/b611278a

An immunoassay based upon photoluminescent gold quantum dots aimed at detecting human IgG in aqueous solution from micromolar to nanomolar concentrations is described.

Herein, we present the proof-of-concept of an immunoassay platform based on photoluminescence quenching of dendrimer-encapsulated gold quantum dots conjugated to an affinity reagent. Due to higher sensitivity, better dynamic range, and potential for easy multiplexing, fluorescence based technology is rapidly gaining popularity from photometry and radio chemistry in various forms of *in vitro* diagnostic (IVD) assays. The consequence of higher sensitivity is in lowering the detection threshold, ultimately reaching the "holy grail" of single cellular and single molecular diagnostics, with the highest promise of achieving this goal coming from applications of quantum dots (QDs).[1,2]

QDs allow the design of tests for new, more efficient biomarkers, which are not accessible with traditional colorimetric methods due to their low concentrations in analytes. They also allow color-coded multiplexing, and thus interrogation of several markers from the same sample volume. Furthermore, the increased sensitivity of the luminescence based tests, compared with photometric assays, leads to a rapid decrease in the sample volume size, which is of special importance in certain applications where the available sample volume is critical.

Recently, small metallic photoluminescent clusters, synthesized using poly(amido) amine (PAMAM) dendrimers as a surface stabilizing agent have been described.[3,4] By utilizing dendrimers of different generations and adjusting the metal to dendrimer concentration ratio, it was reported that it is possible to control the Au quantum dot size[3,4] thus, the photoluminescent properties.

In a recent article, PAMAM dendrimer encapsulated, high quantum yield, size tunable gold quantum dots have been reported with emission wavelengths varying from the ultraviolet to the near infrared.[4] These novel particles have both discrete and narrow absorption and emission bands differing from the semiconductors particles which, in general, absorb light over a broad range of wavelengths in the visible spectrum. Use of second generation hydroxyl terminated PAMAM dendrimer as a surface stabilizing agent provides solubility characteristics ideal for aqueous environments, a means for further functionalization, and minimal size increase.[5] PAMAM dendrimers, especially those of higher generation, have also been used extensively for *in vitro* biological applications due to their membrane permeation ability.[6,7] Photoluminescent characteristics of QDs are greatly affected by surface passivation and surface interactions allowing them to function as immunofluorescence sensors, wherein, for this application, the antigen–antibody immunocomplex formation induces changes in the surface electrostatic properties.

Here we report the synthesis, general conjugation strategy for biomolecules (Fig. 1), high resolution transmission electron microscopy (HRTEM), and atomic force microscopy (AFM) characterizations of a complex composed of AuQDs encapsulated by second generation PAMAM dendrimers conjugated electrostatically to an antibody aimed as a major component of the immunofluorescent assay. As a proof-of-concept, herein we present the immunoassay for the detection of the human IgG antigen, based on the polyclonal, goat-derived anti-human IgG antibody. The same techniques can be applied to other analytes by selecting the appropriate analyte-specific antibody, or in the case of a molecular diagnostics probe, by selecting the proper nucleic acid or peptide sequence for conjugation. While it has been shown that PAMAM dendrimers do fluoresce,[8] the intensity is only substantial at low pH levels. The work presented is conducted at

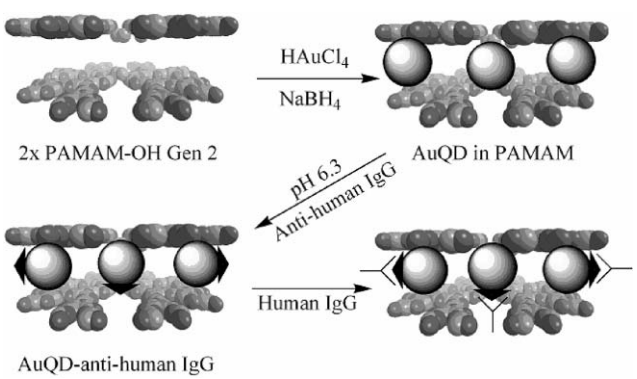

Fig. 1 Schematic representation of PAMAM–OH dendrimer, generation 2, AuQD formation between dendrimers, Conjugation of anti-human IgG (▲) to the AuQD–PAMAM complex, and addition of human IgG (Y) to the system.

[a]*University of Miami, Department of Chemistry, 1301 Memorial Drive, Coral Gables, FL 33146, USA. E-mail: rml@miami.edu*
[b]*MP Biomedicals LLC (Formerly ICN Biomedicals, Inc.), 15 Morgan, Irvine, CA 92618, USA. E-mail: mmicic@mpbio.com*
[c]*Physics Department, Trinity College, Dublin, 2, Ireland*
[d]*Veeco Instruments Inc, 112 Robin Hill Road, Santa Barbara, CA 3117, USA*
[e]*Department of Chemical Engineering and Materials Science, University of California at Irvine, 916 Engineering Tower Irvine, CA 92697-2575, USA*

† Electronic supplementary information (ESI) available: Materials, methods, AFM, control experiment, and Stern–Volmer plot. See DOI: 10.1039/b611278a

a pH of 6.3, therefore the fluorescence of the dendrimer does not contribute to the observed photoluminescence of the AuQDs.

There are various hypotheses as to how the QDs or analogous metallic nanoparticles are stabilized by the dendrimer, however, no one scenario has been proven. There are two main possibilities that are believed to take place. First, the AuQDs may be truly encapsulated within the void spaces of a dendrimer molecule.[9,10] In this case, it would be impossible for more than one QD to be encapsulated within a dendrimer due to the physical constraints of our system. However, it is possible using dendrimers of higher generation.[11] The second possible scenario is that the QDs are sandwiched in the void formed between dendrimer molecules;[12] it is the belief of the authors that this is the type of stabilization that takes place. Although we have no conclusive evidence to support this, our experimental results shown below favor the latter of the two hypotheses.

From the AFM micrograph of the synthesized gold nanoparticles (supporting information, Fig. S1†) we can observe a heterogeneous distribution of the AuQD–PAMAM size. The complex, in general, is an oval and irregular shape. The average size of the AuQD–PAMAM complex determined by measurement of the structure height is 4.9 nm. From HRTEM of the AuQD–PAMAM complex, the average diameter is 4.8 nm (sample size of 100). Absorption measurements show no surface plasmon band at 520 nm (Fig. 2A) indicating that the core AuQDs are 2 nm or smaller[13,14] in diameter, neglecting the dendritic PAMAM organic capping layer, while the entire system, or complex, (dendrimer and AuQD; AuQD–PAMAM) is 4.9 nm. The main absorption band around 300 nm corresponds to that of the pure dendrimer.[15] These

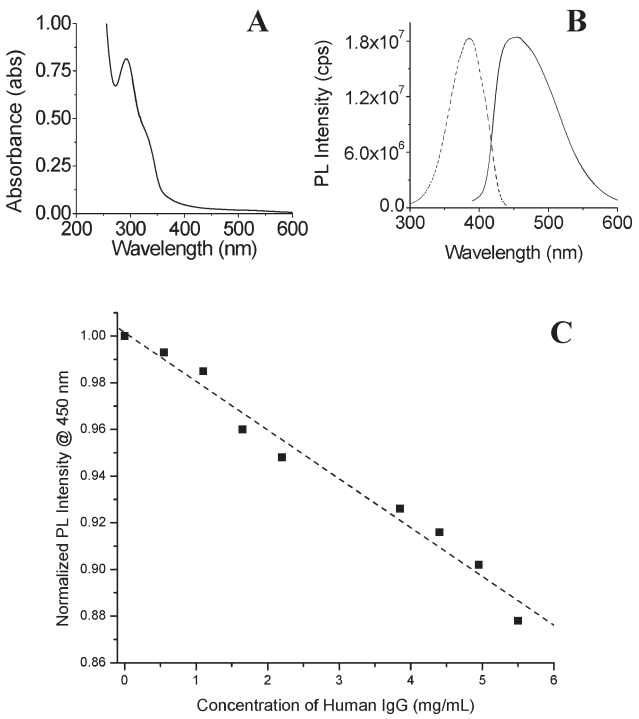

Fig. 2 (A) Absorption spectrum of AuQDs, 1 cm cell pathlength; (B) Excitation and emission spectra of AuQDs in aqueous solution, 1 cm cell pathlength, pH = 6.3: excitation (- -) and emission (–) (C) Quenching of AuQDs conjugated with goat-derived polyclonal anti-human IgG PL with increasing concentration of human IgG.

results are consistent with HRTEM measurements giving an average complex size of 4.8 nm with 80% found to have a diameter between 4 and 6 nm for the pure AuQDs and dendrimer (not coupled to IgG), also agreeing with calculations considering the increase in size[15] due to the PAMAM dendrimer. This size distribution emphasizes one of the key advantages of this system; namely, the overall size of the sensing system is small in comparison to other known methods of detection such as the use of the adaptor proteins biotin and avidin[16] where the introduction of additional proteins vastly increases the size of the system.

Until today, gold nanoparticles have only been used as a staining and reflectometric reagents,[17] and are much larger in size, typically on the order of 20–150 nm. These large nanoparticles are good contrast agents for microscopic techniques; however, they are not useful as photoluminescent particles.

Photoluminescence characterization revealed excitation and emission maxima of pure AuQDs at 387 and 450 nm, respectively (Fig. 2B) which correspond to the published values.[3] After electrostatically coupling the AuQDs to goat-derived polyclonal anti-human IgG, the excitation and emission maxima were unchanged. Human IgG was then introduced and AuQD conjugate photoluminescence intensity was found to decrease with increasing concentrations of human IgG antigen (Fig. 2C). As up to two antigen molecules may bind to one molecule of antibody direct interaction between AuQDs and the quenching complex formed, along with the agglutination process, readily account for the decrease in photoluminescence intensity. The relationship is linear in nature over micromolar to nanomolar ranges, thus allowing easy construction of quantitative immunofluorescence assays and biosensors. Linear regression was performed on the data from the quenching study giving an equation of [IgG] = $-1.12 \times 10^5 x + 1.63 \times 10^7$, (wherein x is photoluminescence signal in counts per second) with a correlation coefficient of r = 0.99. Control measurements involving the titration of human IgG to the AuQD–PAMAM complex (no anti-human IgG) show no decrease in intensity of luminescence as a function of human IgG concentration (supporting information, Fig. S2†).

As the particles are synthesized in the presence of dendrimer, in some instances in the HRTEM micrograph we can still observe the dendrimer encapsulation of the particles. HRTEM reveals that the particles have a uniform internal structure. Fig. 3A represents the micrography of the Au nanoparticles, electrostatically conjugated with goat polyclonal anti-human IgG antibody. Due to the low electron contrast, the organic coating can be only observed as a sporadic halo on the particles. The particles take up a random orientation occasionally forming small clusters of particles. After addition of the recombinant human IgG protein, the agglomeration of functionalized nanoparticles occurs as depicted in the HRTEM micrography of Fig. 3B. The agglomeration occurs due to the existence of two binding sites of antibodies for antigens and as such can be exploited for immunoturbidity or immunoprecipitation assay.

While discriminating the dendrimer from the AuQDs in absolute terms using HRTEM is difficult, what can be visualized is the difference in density of the organic PAMAM component from the inorganic AuQDs. As can be seen in Fig. 3C there is a clear difference between the density of the QDs from that of the PAMAM dendrimer matrix. In this figure, at least four

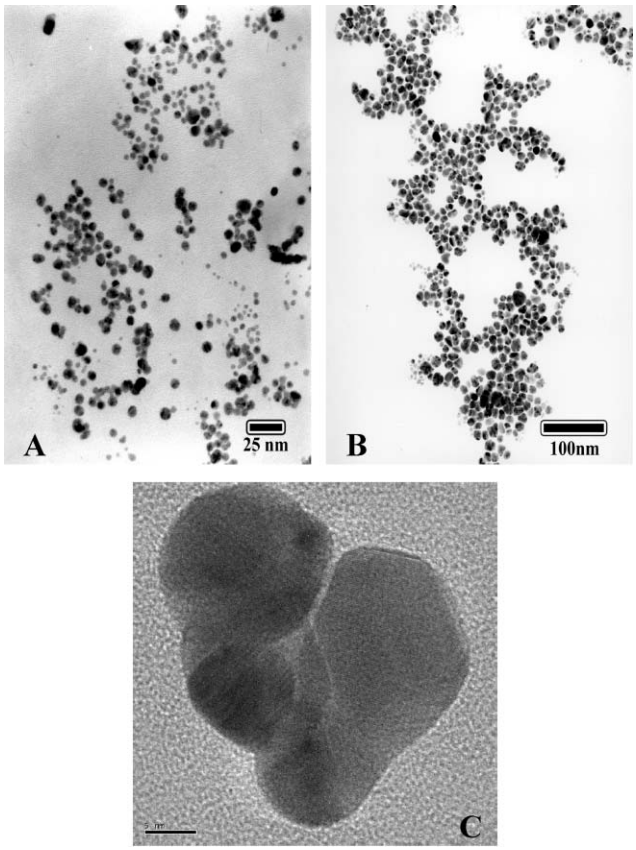

Fig. 3 (A) HRTEM micrograph of AuQD–antibody conjugates, data bar size 25 nm (B) HRTEM micrograph of the complex agglomerate formed after addition of recombinant human IgG protein to the AuQD-antibody conjugate, data bar size 100 nm. (C) HRTEM micrograph of AuQD–antibody conjugates showing density differences due to PAMAM and Au, data bar size 5 nm.

AuQD–PAMAM complexes are seen agglomerated together due to the low vacuum conditions required for HRTEM. The PAMAM matrix appears less dense, or lighter, than does the more dense, or darker, AuQDs. The AuQDs appear to be randomly distributed and due to the resolution of the microscope are not fully resolved in all instances. The fact they are randomly distributed, and not always found in the same relative position when compared to the dendrimer matrix leads the authors to believe that there is a sandwiching stabilization effect. The diameter of the dendrimer complex appears to be about 5 nm, while the AuQDs themselves are less than 2 nm.

The presented proof-of-concept immunofluorescence assay is capable of detecting concentrations of antigen over a wide dynamic range from millimolar to nanomolar levels. The AuQD–PAMAM complex, its antibody conjugate, and immunocomplex formed after addition of antigen were topographically characterized by AFM and HRTEM microscopies, and spectroscopically characterized by UV-vis and luminescence. Herein, we confirm the linear relationship between photoluminescence quenching of the conjugate with addition of antigen, with a broad dynamic range, a necessary ingredient for any *in vitro* assay or biosensor. Due to the relatively large size of IgG and the immunocomplex formed with its goat-derived antigen compared to the AuQDs, and not neglecting agglutination, the most probable mechanism of luminescence quenching is static quenching supported by a linear Stern–Volmer plot (supporting information, Fig. S3†) with a Stern–Volmer constant of 2.28×10^{-2} mg^{-1} mL^{-1}; this relatively low value indicates partial steric shielding, as seen in Fig. 1, of the AuQDs by the PAMAM dendrimer.

This work was supported by National Science Foundation (CHE-0416095).

The authors would like to gratefully acknowledge Jhony Orbulescu for his insightful discussions.

Notes and references

1 (*a*) K. K. Jain, *Clin. Chim. Acta*, 2005, **358**(1–2), 37054; (*b*) P. Fortina, L. J. Kricka, S. Surrey and P. Grodzinski, *Trends Biotechnol.*, 2005, **23**(4), 168–173; (*c*) K. K. Jain, *Expert Rev. Mol. Diagn.*, 2003, **3**(2), 153–161.
2 (*a*) X. Michalet, F. F. Pinaud, L. A. Bentolila, J. M. Tsay, S. Doose, J. J. Li, G. Sundaresan, A. M. Wu, S. S. Gambhir and S. Weiss, *Science*, 2005, **307**(5709), 538–544; (*b*) M. A. Hahn, J. S. Tabb and T. D. Krauss, *Anal. Chem.*, 2005, **77**(15), 4861–4869; (*c*) M. Kuno, D. P. Fromm, H. F. Hamann, A. Gallagher and D. J. Nesbitt, *J. Chem. Phys.*, 2001, **115**(2), 1028–1040; (*d*) M. Seydack, *Biosens. Bioelectron.*, 2005, **20**(12), 2454–2469.
3 J. Zheng, J. T. Petty and R. M. Dickson, *J. Am. Chem. Soc.*, 2003, **125**, 7780–7781.
4 J. Zheng, C. Zhang and R. M. Dickson, *Phys. Rev. Lett.*, 2004, **93**(7), 077402.
5 C. Crooks, S. Lemon and Z. Yeung, in *Metal Nanoparticles: Synthesis, Characterization, and Applications*, ed. D. L. Feldheim and C. A. Foss, Marcel Dekker Ltd, New York, 2002, Chapter 11.
6 J. Khandare, P. Kolhe, O. Pillai, S. Kannan, M. Lieh-Lai and R. M. Kannan, *Bioconjugate Chem.*, 2005, **16**(2), 330–337.
7 A. S. Chauhan, N. K. Jain, P. V. Diwan and A. J. Khopade, *J. Drug Targeting*, 2004, **12**(9–10), 575–583.
8 D. Wang and T. Imae, *J. Am. Chem. Soc.*, 2004, **126**, 13204–13205.
9 H. Lang, S. Maldonado, K. J. Stevenson and B. D. Chandler, *J. Am. Chem. Soc.*, 2004, **126**, 12949–12956.
10 J. C. Garcia-Martinez and R. M. Crooks, *J. Am. Chem. Soc.*, 2004, **126**, 16170–16178.
11 F. Grohn, G. Kim, B. J. Bauer and E. J. Amis, *Macromolecules*, 2001, **34**, 2179–2185.
12 M. Ujihara, J. Orbulescu, T. Imae and R. M. Leblanc, *Langmuir*, 2005, **21**, 6846–6854.
13 R. M. Crooks, M. Zhao, L. Sun, V. Chechik and L. K. Yeung, *Acc. Chem. Res.*, 2001, **34**, 181–190.
14 K. Esumi, A. Suzuki, N. Aihara, K. Usui and K. Torigoe, *Langmuir*, 1998, **14**, 3157–3159.
15 J. Zheng and R. M. Dickson, *J. Am. Chem. Soc.*, 2002, **124**, 13982–13983.
16 J. K. Jaiswal, E. R. Goldman, H. Mattoussi and S. M. Simon, *Nat. Methods*, 2004, **1**, 73–78.
17 N. T. K. Thanh and Z. Rosenzweig, *Anal. Chem.*, 2002, **74**, 1624–1628.

